Dyes and Pigments 136 (2017) 46–53

Contents lists available at ScienceDirect

Dyes and Pigments

journal homepage: www.elsevier.com/locate/dyepig

Synthesis and characterization of novel thieno[3,2-*b*]thiophene based metal-free organic dyes with different heteroaromatic donor moieties as sensitizers for dye-sensitized solar cells

Sara S.M. Fernandes [a], M. Cidália R. Castro [a], I. Mesquita [b], L. Andrade [b], A. Mendes [b], M. Manuela M. Raposo [a, *]

[a] Centro de Química, Universidade do Minho, Campus de Gualtar, 4710-057, Braga, Portugal
[b] LEPABE - Faculdade de Engenharia, Universidade do Porto, rua Dr. Roberto Frias, 4200-465, Porto, Portugal

ARTICLE INFO

Article history:
Received 22 May 2016
Accepted 8 August 2016
Available online 9 August 2016

Keywords:
Dye sensitized solar cells
Heterocyclic organic dye
Metal-free thieno[3,2-*b*]thiophene dye
Cyanoacetic acid anchoring group
Heterocyclic donor groups
Co-adsorption

ABSTRACT

Four novel heterocycle dyes **3a**-**d** were synthesized in order to study the variations produced in the optical, electronic and photovoltaic properties by substitution of different electron-rich heterocyclic groups to the thieno[3,2-*b*]thiophene system. The final push-pull conjugated dyes **3a**-**d** were synthesized by Suzuki-Miyaura coupling reaction followed by Knoevenagel condensation of the corresponding aldehyde precursors with cyanoacrylic acid **2a**-**d**. These new push-pull systems are based on a thieno[3,2-*b*]thiophene spacer, a cyanoacetic acid anchoring group and several electron-rich heterocycles (thiophene, pyrrole and furan) as donor groups. The multidisciplinary study concerning the optical, redox and photovoltaic characterization of the dyes reveals that compound **3b** bearing a hexyl-bithiophene donor group/heterocyclic spacer exhibits the best overall conversion efficiency (2.49%) as sensitizer in nanocrystalline TiO_2 dye sensitized solar cells. Co-adsorption studies between **N719** and **3b** revealed that upon addition of **N719** co-adsorbent, the optimized cell efficiencies were improved by 16–77%. The best efficiency was 4.40%, corresponding to 54% of the photovoltaic performance of the **N719**-based DSSC fabricated and measured under similar conditions.

1. Introduction

Modern civilization is reliant on energy resources, like non-renewable fossil fuels. As such, in the last decades we observed a greater focus on renewable energy sources and sustainable development in order to diminish the greenhouse effect and ensure economic growth. Solar energy is a very interesting energy source due to its inexhaustibility, cleanness, and the capacity to be converted directly into electrical power by photovoltaic cells devices. Consequently, among several new technologies, solar cells based on dye sensitizers (DSSCs) adsorbed on nanocrystalline TiO_2 electrodes have received significant attention, mainly because of their high incident solar light-to-electricity conversion efficiency. The light absorber or dye sensitizer is a crucial element since it plays an important role on the conversion efficiency as well as on the stability of the devices. Therefore, dyes are required to fulfil some essential characteristics, such as having a push-pull structure, broad spectral response (visible and near-infrared region), photostability, controlled aggregation and recombination, proper electronic energies (HOMO, LUMO), good intramolecular charge transfer, and an anchoring group to strongly bind onto the semiconductor surface [1–3].

Dye sensitizers applied in solar cells were mainly ruthenium complexes, consisting of the central metal ion with organic ligands containing an anchoring group. The best photovoltaic performances both in terms of conversion yield and long term stability, with efficiencies surpassing 11%, have been achieved by polypyridyl complexes of ruthenium. However, ruthenium is a trace element on top of being a heavy metal, and its lack of abundance in nature, in addition with the latent risk to the environment, complicated synthetic processes and difficult purification of the dyes, makes Ru-based dye sensitizers not suited in terms of cost efficiency and environmental friendliness. Nevertheless, transition metal complexes are still playing a role in DSSC development [1].

Metal free sensitizers such as organic dyes and natural dyes

* Corresponding author.
E-mail address: mfox@quimica.uminho.pt (M.M.M. Raposo).

http://dx.doi.org/10.1016/j.dyepig.2016.08.020
0143-7208/

have received attention as an alternative DSSC applications and have been extensively developed as convenient substitutes to metal-based dyes as a result of their high molar extinction coefficient, simple synthesis and purification routes, diversity in molecular structures which offers infinite possibilities to tune the photophysical and electrochemical properties, colourful and decorative natures, low cost and environmental friendliness. The molecular structure for efficient metal free organic dyes generally used is a donor – π-bridge – acceptor (D-π-A) system that promotes efficient charge transfer from the ground state to the excited state. As a result, in the last two decades, a wide range of structural modifications to the donor or acceptor group and π-bridge have been implemented for the preparation of organic chromophores with high performance for DSSCs [1d,3]. It is well known that the structure of the organic dye (donor group, π-spacer and acceptor/anchoring group) has profound repercussions on the performance as sensitizers for DSSC. Common donors groups are *N*,*N*-dialkylamine, triphenylamine, carbazole, indoline, etc. The electronic nature, the length of conjugation and the planarity of the π-spacer are other important factors for an efficient charge separation and can be addressed by modifying the π-bridge. π-Bridges are usually composed of electron rich heterocycles (pyrrole, thiophene, furan), by ethene, ethine, or benzene units. The acceptor/anchoring group is also an important part in DSSCs being the carboxylic acid (-COOH) the standard anchoring group for sensitizers due to its relative stability and easy synthesis, and is typically used in the form of a cyanoacetic acid [3]. Nevertheless, other groups are also commonly developed, such as rhodanine-3-acetic acid, phosphoric acid, sulfonic acid, acetic anhydride, ester, acid chloride pyridine, aldehyde etc. Results have shown that rhodanine-3-acetic acid as an anchoring group leads to a significant bathochromic shift due to the extension of the π-conjugation system, however cyanoacrylic acid favours better properties of DSSCs, not only due to its coplanarity with respect to spacer unit and good electron coupling with TiO_2, but also because the LUMO level of rhodanine-3-acetic acid based dyes is centred on the carbonyl and thiocarbonyl groups (DFT calculations) which results in the position of the LUMO being isolated from the −COOH anchoring group due to the presence of the methylene moiety [4]. The first metal free organic dyes used as sensitizers for DSSCs exhibited very poor performances, but since then numerous dyes have been developed and their devices showed good photovoltaic performance, which achieved similar efficiencies compared to those of Ru complexes (12%) [5a-k]. More recently Yano Hanaya and collaborators reported a high conversion efficiency of over 14% using collaborative sensitization between two organic dyes bearing two different anchoring groups an alkoxysilyl and a carboxy moiety [5l].

The most efficient DSSCs, very frequently, contain thiophene units, (*e.g.* oligothiophenes, fused thiophenes, alkylenedioxythiophenes, etc.) due to their excellent charge-transport properties. Additionally, thienothiophene derivatives offers better π-conjugation and smaller geometric relaxation energy upon oxidation when compared to bithiophene [3,5,6]. Furthermore, the introduction of sterically hindered alkyl chains in the dye structure is expected to suppress the aggregation tendency which allow best photovoltaic performances [5g].

Having in mind the work reported before in this area as well as our experience on the synthesis and characterization of push-pull heterocyclic π-conjugated systems for several optical applications [7], we report in this manuscript the synthesis and evaluation of four novel push-pull organic dyes bearing electron-rich heterocyclic groups (thiophene, *n*-hexyl-2,2′-bithiophene furan and pyrrole) as donor groups/π bridges, a thienothiophene as spacer group, and a cyanoacetic acid as the acceptor/anchoring moiety.

2. Results and discussion

2.1. Synthesis and characterization

A series of heterocyclic dyes were designed in order to study the effect of different donor moieties (different electron-rich heterocycles) in their optical, redox and photovoltaic properties. All designed π-conjugated systems were functionalized with the cyanoacetic acid group, due to the best efficiency of this acceptor/anchoring group in DSSCs [4]. As π-bridge/spacer we employed the thieno[3,2-*b*]thiophene, not only because of the great charge transfer properties of thiophene but also due to the superior π-conjugation and low geometric relaxation energy upon oxidation of the this conjugated system [6a-d,g,7]. Instead of the "classical" donor groups we used electron-rich heterocycles such as thiophene, pyrrole and furan having in mind that they can have a dual role as electron donor groups and as π-spacers [7c,7g,8].

The precursor aldehydes **2a-d** were prepared, in fair to excellent yields (26–84%), by Suzuki-Myiaura coupling of 5-bromothieno[3,2-*b*]thiophene-2-carbaldehyde **1** with commercially available heterocyclic boronic acids. The final push-pull conjugated dyes **3a-d** were synthesized by Knoevenagel condensation of the corresponding aldehyde precursors **2a-d** with cyanoacetic acid in refluxing ethanol, using piperidine as catalyst (Scheme 1, Table 1). The novel dyes **2**–**3** were completely characterized by the usual spectroscopic techniques.

2.2. Study of the optical properties

The UV–Vis spectra of dyes **3** in ethanol at room temperature are provided in Fig. 1. All dyes exhibit a strong and broad band between 364 and 433 nm that can be assigned to an internal charge transfer process (ICT) between the donor and acceptor groups, which depends on the heterocyclic group linked to the thienothiophene spacer [10]. The addition of a 2-hexylthiophene unit, as seen in dye **3b**, induces a bathochromic shift in the longest wavelength absorption of 34 nm compared with dye **3a**. This result can be explained having in mind that the incorporation of an additional thiophene ring increases the charge transfer properties in a push-pull compound due to the bathochromic effect of sulphur, the partial decrease of aromatic character of the thiophene heterocycle, and the increase of the conjugation [8b,10]. On the other hand, compound **3d**, having a *N*-methyl pyrrole donor unit exhibits a 65 nm hypsochromic shift of absorption maxima compared to compound **3a** functionalized with a thiophene donor moiety. That can be explained by realizing that the pyrrole electron pair is involved in the aromatic system and, thus, not available for delocalization to the cyanoacetic acceptor group resulting in an increased energy gap between HOMO and LUMO orbitals [7a,9,10,11].

The novel synthesized push-pull dyes **3a-c** have higher molar extinction coefficients (23,315-25666 M^{-1} cm^{-1}) when compared to the standard ruthenium dyes **N3** (13,900 M^{-1} cm^{-1}) [12] and **N719** (14,000 M^{-1} cm^{-1}) [13].

Dyes **3** were excited at the wavelength of maximum absorption, at room temperature, in order to study their fluorescence properties (Fig. 2). With the exception of dye **3b**, all dyes showed weak emissive properties, with relative fluorescence quantum yields ranging from 0.015 to 0.021. As expected, due to an extension of the conjugated π-system, we observed an increase in the fluorescence quantum yield when a second thiophene unit was introduced [14]. (**3a**, $\phi_F = 0.020$; **3b**, $\phi_F = 0.356$).

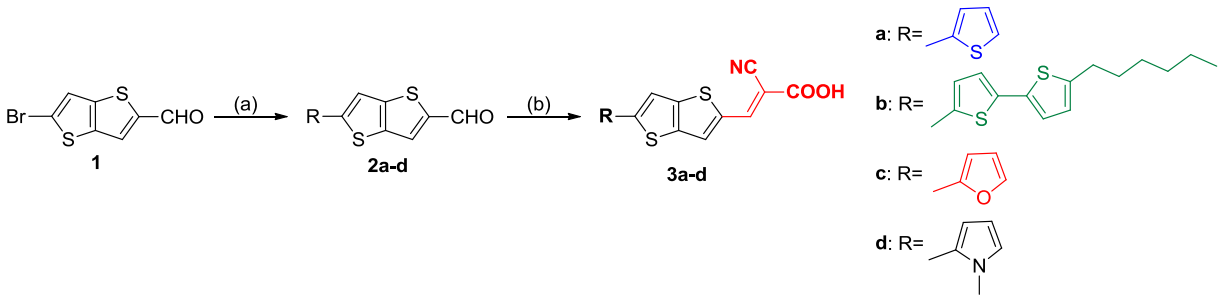

Scheme 1. Reagents and conditions: (a) DME, $Pd(PPh_3)_4$, N_2, EtOH, Na_2CO_3; (b) cyanoacetic acid, piperidine, EtOH, reflux.

Table 1
Yields, UV–visible, Fluorescence, IR and ^{1}H NMR data of compounds **2**–**3**.

Cpd	Yield (%)	UV–vis[a]		Fluorescence[a]			IR[b]			^{1}H NMR[c]			
		λ_{max} (nm)	ε (M^{-1} cm^{-1})	λ_{em} (nm)	Stokes shift (nm)	ϕ_F	ν (cm^{-1})			δ (ppm)			
							C=O	OH	CN	*CHO*	*H3*	*H3′*	*H6′*
2a	79	371	15,358	460	89	0.574	1667	–	–	9.94	–	–	–
2b	76	413	17,000	556	143	0.938	1661	–	–	9.94	–	–	–
2c	26	371	22,390	466	95	0.565	1650	–	–	9.94	–	–	–
2d	84	326	16,470	470	144	0.013	1652	–	–	9.94	–	–	–
3a	68	399	23,315	476	77	0.020	1634	3426	2190	–	8.12	7.76	7.98
3b	43	433	25,666	527	94	0.356	1642	3423	2208	–	8.39	7.81	8.17
3c	24	398	24,348	469	71	0.015	1639	3428	2217	–	8.13	7.77	8.00
3d	11	364	5996	471	107	0.021	1638	3411	2213	–	8.13	7.58	7.96

[a] All the UV–Vis and fluorescence spectra were performed in ethanol, using DPA as a quantum yield standard, except for compounds **2b** and **3b** where rhodamin-6G was used.
[b] IR spectra were performed in Nujol for compounds **2a**-**d** and dichloromethane liquid film for compounds **3a**-**d**.
[c] For compounds **2a**-**c**, ^{1}H NMR was performed at 400 MHz, using $CDCl_3$ as solvent, and for compounds **2d** and **3a**-**d**, ^{1}H NMR was performed at 400 MHz, using DMSO-d_6 as solvent.

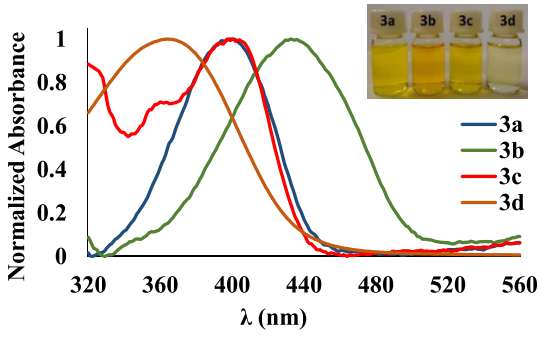

Fig. 1. Normalized absorption spectra of dyes **3** in ethanol (λ_{max}: **3a** = 399 nm; **3b** = 433 nm; **3c** = 398 nm; **3d** = 364 nm).

2.3. ^{1}H NMR study

The comparative electron donating strength of the donor moiety can be assessed by examining the ^{1}H NMR spectra for the chemical shifts of 3′-H, which is the closest located proton relative to the donor group. A stronger electron donating ability of the donor moiety will improve the internal charge transfer (ICT) in the push-pull system, moving the electron density towards the acceptor end group, which leads to a downfield of 3′-H (higher chemical shift). Dye **3b**, functionalized with a 5-hexyl-2,2'-bithiophene unit, presents the highest chemical shift for the 3′-H at 7.81 ppm, meaning the strongest electron donor effect, while dyes **3a** and **3c** show the equivalent proton located at 7.76 and 7.77 ppm, respectively. For dye **3d**, 3′-H is the most upfield positioned for all dyes (7.58 ppm) due to the large contribution of the non-ligant electrons at the nitrogen atom that stabilizes the donor ring, and consequent lower electron push [7c,9,11].

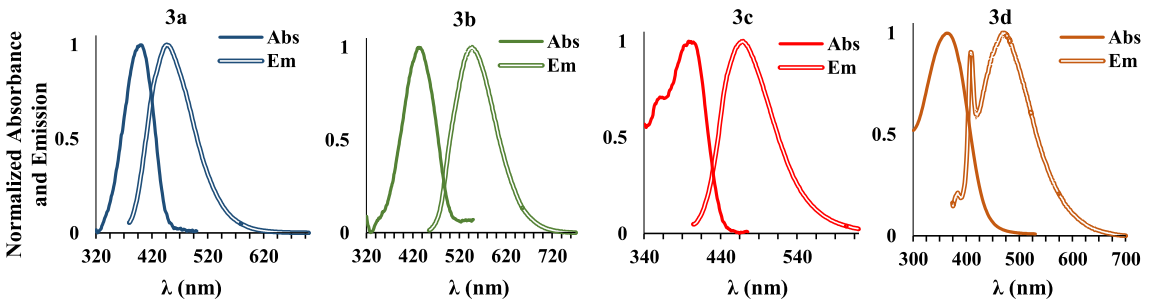

Fig. 2. Normalized absorption and emission spectra for dyes **3**, in ethanol.

2.4. Electrochemical study

Cyclic voltammetry is a widely used technique to obtain HOMO and LUMO energy levels of a compound. It is well known that the position of the HOMO and LUMO of the heterocyclic dye used as sensitizer in DSSCs affects their photovoltaic performance. The electronic nature of the heteroaromatic rings in the π-bridge affects significantly the oxidation potential values. Therefore, heterocyclic systems bearing more electron rich heterocycles are easier to oxidize due to the stronger electron-donating ability of the system resulting in a higher HOMO energy level (estimated from its first oxidation potential) [9,10].

In order to get a bigger inside to the electronic properties of compounds **3a**-**b**, which exhibit the best photovoltaic performances, we performed an electrochemical study by cyclic voltammetry and the results can be found in Table 2. Both dyes display a reversible oxidation process at +0.90 V for **3a** and +0.65 V for **3b** which are more positive than the iodine redox potential (0.42 V). This is an important issue having in mind that an oxidation potential higher than that of redox potential of iodine couple is necessary to reduce the backward electron transfer to electrolyte solution in DSSCs. These results reveal that, the dispositive could show a good performance because of its higher difference with the iodide/triiodide redox couple and then, a better regeneration of the oxidized dye after electron injection into the conduction band of TiO_2 [15].

Upon reduction, the dyes exhibit waves at −1.68 V for **3a** and −2.01 V for **3b**. The addition of a second thiophene heterocyclic in the donor moiety/π-spacer in compound **3b** lowered the half-wave potential of the oxidation wave [16] but not the reduction wave, resulting in a broader bang gap (2.58 eV for **3a** and 2.70 eV for **3b**).

2.5. Photovoltaic performance of DSSCs

Table 3 and Fig. 3 present the performance parameters (short-circuit current density, J_{SC}; open circuit voltage, V_{OC}; fill factor, *FF*; and efficiency, η) of the prepared DSSCs sensitized with **3a-d** dyes, as well as the standard ruthenium-dye **N719** for comparison.

Dyes **3a**, **3c** and **3d** bearing one thiophene, furan or pyrrole heterocycle, linked to the thieno[3,2-*b*]thiophene spacer, exhibit very low photovoltaic performances with efficiencies in the range of 0.04–0.22%. The thiophene derivative **3a** exhibits a higher value compared to **3c** and **3d** which is in accordance with their optical and electronic properties [7a-c,9,11]. In contrast, dye **3d** exhibits the lowest performance of all dyes ($\eta = 0.04\%$) which could be due to the higher HOMO energy values for the compounds bearing this electron-rich heterocycle [9].

On the other hand, dye **3b** shows the best performance of all dyes, presenting an efficiency of 2.49%, with a J_{SC} of 6.92 mA/cm^2 and a V_{OC} of 0.550 V. This efficiency value represents ca. 30% of the power conversion efficiency generated by the reference DSSC using **N719** dye. The increased photocurrent density observed for dye **3b**, when compared to dye **3a**, should be ascribed to the incorporation of an additional thiophene π-bridging unit that when incorporated in a push-pull compound enhances their charge transfer properties and induces a bathochromic shift on the absorption spectrum toward longer wavelengths [3,16a].

The long hexyl hydrocarbon chain linked to the bithiophene donor moiety/π-spacer will improve also the solubility of the dye suppressing the dark current by blocking electrolytes from close contact with the TiO_2 surface [3,5g,17]. Therefore, the higher open-circuit voltage of compound **3b** may be due to a decreased electron recombination with triiodide redox pair.

DSSCs with ruthenium-based dyes yield maximum efficiencies by using thick TiO_2 films due to low molar extinction coefficients (<20,000 M^{-1} cm^{-1}) credited to the metal-to-ligand charge transfer molecular excitation. On the other hand, organic dyes commonly have higher molar extinction coefficients, which allows for thinner films and reduction of charge transport loss [5g], but displays narrow absorption bands decreasing the light harvesting ability [1,3]. For better understanding the performance difference between reference DSSC (with **N719** dye) and the ones prepared with push-pull thieno[3,2-*b*]thiophene **3a-d** derivatives, and in order to combine the different advantages of both dye families, co-adsorption was performed between **N719** and **3b** dye which exhibit

Table 3
Photovoltaic performance of DSSCs based on dyes **3** and dye **N719**.

Dye	V_{OC} (V)	J_{SC} (mA/cm^2)	*FF* (%)	η (%)
3a	0.450	0.75	0.629	0.22
3b	0.550	6.92	0.653	2.49
3c	0.400	0.24	0.614	0.06
3d	0.350	0.20	0.485	0.04
N719	0.750	15.58	0.692	8.09

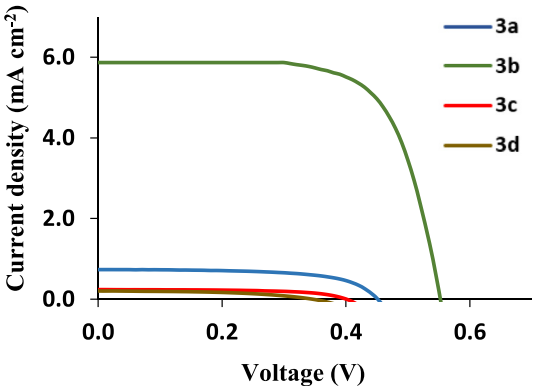

Fig. 3. Photocurrent density-voltage characteristics of the devices prepared with dyes **3a-d**.

Table 2
Electrochemical data of synthesized dye **3b** and dye **N719**.

Dye	Reduction[a]			Oxidation[a]	E_{HOMO}[b] (eV)	E_{LUMO}[b] (eV)	Band gap[c] (eV)
	$-^1E_{pc}$ (V)	$-^2E_{pc}$ (V)	$-^3E_{pc}$ (V)	$^1E_{pa}$ (V)			
3a	1.68	2.78	–	0.90	−5.29	−2.71	2.58
3b	2.01	2.46	2.81	0.65	−5.04	−2.34	2.70
N719	2.04	2.52	2.99	0.46	−4.85	−2.35	2.50

[a] Measurements made in dry DMF containing 1.0 mM in each compounds and 0.1 M $[NBu_4][BF_4]$ as base electrolyte at a carbon working electrode with a scan rate of 0.1 V s^{-1}. All E values are quoted in volts *vs* the ferrocenium/ferrocene-couple. E_{pc} and E_{pa} correspond to the cathodic and anodic peak potentials, respectively.
[b] $E_{HOMO} = -(4.39 + E_{ox})$ (eV) and $E_{LUMO} = -(E_{red} + 4.39)$ (eV).
[c] Calculated form the difference between the onset potentials for oxidation and reduction.

the best photovoltaic performance. Co-adsorption with different dyes covering a larger visible spectral region might be an effective and economic way to increase the efficiency of the solar cells but also might be very useful in the aggregates suppression usually observed on these systems. The correspondent photovoltaic performance results are presented on Table 4. For the five proportions prepared (100% **N719** - 0% **3b**, 75% **N719** - 25% **3b**, 50% **N719** - 50% **3b**, 25% **N719** - 75% **3b**, 0% **N719** - 100% **3b**) it is noticed that J_{SC} decreases almost linearly with **3b** dye percentage, explained by the decrease on the absorption peak of **N719** dye at 530 nm (Fig. 4). On the other hand, the variation on the V_{OC} is more visible for the percentage 100% **N719** - 0% **3b** (Fig. 5). This means that when **3b** dye is used, the back electron transfer is favoured since the iodide/triiodide electrolyte has a better access to the electrons on the TiO_2 conduction band.

Upon addition of **N719** co-adsorbent, the optimized cell efficiencies were improved by 16–77%. The best efficiency was 4.40%, corresponding to 54% of the photovoltaic performance of the **N719**-based DSSC fabricated and measured under similar conditions.

3. Conclusions

Starting from commercially available precursors as well as by using simple and convenient procedures, novel push-pull thieno[3,2-*b*]thiophenes **3a**-**d** were obtained in fair to excellent yields by Suzuki-Miyaura coupling reaction followed by Knoevenagel condensation of the corresponding aldehyde precursors with cyanoacetic acid **2a**-**d**.

The optical and the redox properties of these push-pull π-conjugated systems can be readily tuned varying the electron donor ability of the heterocyclic donor moiety linked to the thieno[3,2-*b*]thiophene spacer as well as by increasing the π-spacer.

The multidisciplinary study concerning the optical, redox and photovoltaic characterization of the dyes reveals that compound **3b** bearing a 5-hexyl-2,2'-bithiophene donor group/heterocyclic spacer exhibits the best overall conversion efficiency (2.49%) as sensitizer in nanocrystalline TiO_2 dye sensitized solar cells. This result demonstrates that the addition of the second π-bridging thiophene broadens the visible absorption spectra as well as enhances the electron-donating ability of this dye.

Additionally, the introduction of a longer alkyl chain into the bithiophene spacer/donor moiety will retard recombination and the introduction of an additional thiophene as the conjugate bridge will increase the photocurrent response; features which lead to enhanced J_{sc}. Therefore we conclude that the introduction of both hexyl-chain and a thiophene heterocycle into DSSC can improve the cell efficiency significantly.

Consequently, it is expected that, higher efficiency could be achieved for thienothiophene-based metal-free dyes by adjusting the molecular structure of this dyes.

Co-adsorption studies between **N719** and **3b** revealed that upon addition of **N719** co-adsorbent, the optimized cell efficiencies were improved by 16–77%. The best efficiency was 4.40%, corresponding to 54% of the photovoltaic performance of the **N719**-based DSSC fabricated and measured under similar conditions.

Table 4
Photovoltaic parameters of DSC sensitized **3b** dye mixed with **N719** compared with commonly standard cells.

Dye	V_{OC} (V)	J_{SC} (mA/cm^2)	*FF* (%)	η (%)
100% **N719** – 0% **3b**	0.750	15.58	0.692	8.09
75% **N719** – 25% **3b**	0.610	12.25	0.589	4.40
50% **N719** – 50% **3b**	0.580	10.16	0.625	3.68
25% **N719** – 75% **3b**	0.570	8.54	0.595	2.90
0% **N719** – 100% **3b**	0.550	6.92	0.653	2.49

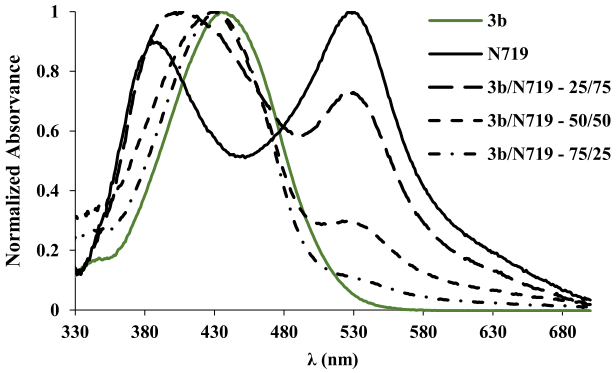

Fig. 4. Normalized absorption spectra of dye **3b** mixed, in different percentages, with **N719** dye, in ethanol.

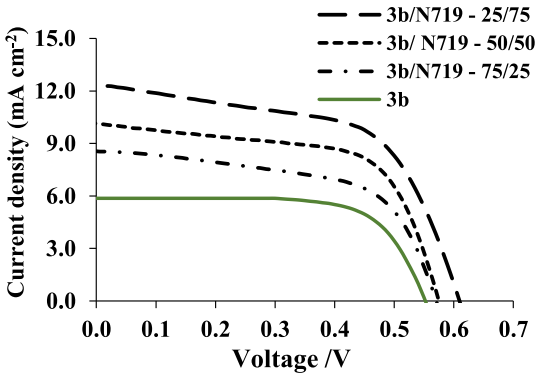

Fig. 5. Photocurrent density-voltage characteristics of the devices prepared with compound **3b** mixed in different percentages with **N719** dye.

4. Experimental

4.1. Materials and methods

2-Thiopheneboronic acid, 5'-hexyl-2,2'-bithiophene-5-boronic acid pinacol ester, 2-furanboronic acid, *N*-methyl-2-pyrroleboronic acid pinacol ester and cyanoacetic acid were purchased from Aldrich. All commercially available reagents and solvents were used as received. 5-Bromo-thieno[3,2-*b*]thiophene-2-carbaldehyde was synthesized using the experimental procedure reported before [5h]. Reaction progress was monitored by thin layer chromatography, 0.25 mm thick precoated silica plates (Merck Fertigplatten Kieselgel 60 F254), and spots were visualised under UV light. Purification was achieved by silica gel column chromatography (Merck Kieselgel, 230–400 mesh). NMR spectra were obtained on a Brucker Avance II 400 at an operating frequency of 400 MHz for ^{1}H and 100.6 MHz for ^{13}C, using the solvent peak as internal reference. The solvents are indicated in parenthesis before the chemical shifts values (δ relative to TMS). Peak assignments were made by comparison of chemical shifts, peak multiplicities and *J* values, and were supported by spin decoupling-double resonance and bidimensional heteronuclear HMBC (heteronuclear multiple bond coherence) and HMQC (heteronuclear multiple quantum coherence) techniques. Melting points were determined on a Gallenkamp apparatus and are uncorrected. Infrared spectra were recorded on a BOMEM MB 104 spectrophotometer. UV–Vis absorption spectra were obtained using a Shimadzu UV/2501PC

spectrophotometer. Fluorescence spectra were collected using a FluoroMax-4 spectrofluorometer. Luminescence quantum yields were measured in comparison with ethanol solution of 9,10-diphenylanthracene (ϕ_F = 0.95) [18], or rhodamine 6G (ϕ_F = 0.95) [19] as standards. Mass spectrometry analysis were performed at the C.A.C.T.I. – Unidad de Espectrometria de Masas of the University of Vigo, Spain.

4.2. Synthesis

4.2.1. General procedure for the synthesis of thieno[3,2-b]thiophene derivatives **2** through Suzuki coupling [20]

5-Bromothieno[3,2-*b*]thiophene-2-carbaldehyde **1** (0.5 mmol, 125 mg) was coupled to heterocyclic boronic acids (0.6 mmol) in a mixture of DME (8 mL), ethanol (2 mL), aqueous 2 M Na_2CO_3 (1 ml) and $Pd(PPh_3)_4$ (5 mol %) at 80 °C, under nitrogen. The reaction was monitored by TLC, which determined the reaction time (24–48 h). After cooling, the mixture was extracted with chloroform (3 × 20 ml) and a saturated solution of NaCl were added (20 mL) and the phases were separated. The organic phase was washed with water (3 × 10 mL) and with 10 mL of a solution of NaOH (10%). The organic phase obtained was dried ($MgSO_4$), filtered, and the solvent removed to give a crude mixture. The crude product was purified through a silica gel chromatography column using mixtures of chloroform and light petroleum of increasing polarity to afford the coupled products **2**. Recrystallization from *n*-hexane/dichloromethane gave the pure compounds.

4.2.1.1. 5-(Thiophen-2'-yl)thieno[3,2-b]thiophene-2-carbaldehyde (**2a**).

Light brown solid (79%). Mp: 155–157 °C. IR (Nujol): 1667, 1532, 1500, 1229, 1163, 1125 cm^{-1} λ_{max}(ethanol)/nm 371 (ε/dm^3 mol^{-1} cm^{-1} 61,650). ^{1}H NMR ($CDCl_3$, 400 MHz) δ 7.08 (1H, dd, J = 5.2 and 3.6 Hz, 4′-H), 7.31 (1H, dd, J = 3.6 and 1.2 Hz, 5′-H), 7.35 (1H, dd, J = 5.2 and 1.2 Hz, 3′-H), 7.39 (1H, d, J = 0.4 Hz, 6-H), 7.87 (1H, d, J = 0.8 Hz, 3-H), 9.94 (1H, s, C*H*O) ppm. ^{13}C NMR ($CDCl_3$, 100.6 MHz) δ 115.95, 125.43, 126.47, 128.22, 128.95, 136.59, 137.59, 144.61, 145.67, 146.51, 182.99 ppm. MS (EI) *m/z* (%) = 250 ($[M]^+$, 100), 249 (46), 221 (18), 176 (23). HMRS: *m/z* (EI) found $[M]^+$ 249.9582; $C_{11}H_6OS_3$ requires $[M]^+$ 249.9581.

4.2.1.2. 5-(5′-(5″-Hexylthiophen-2″-yl)thiophen-2′-yl)thieno[3,2-b]thiophene-2-carbaldehyde (**2b**).

Light orange solid (76%). Mp: 156–158 °C. IR (Nujol): 1661, 1226 cm^{-1} λ_{max}(ethanol)/nm 413 (ε/dm^3 mol^{-1} cm^{-1} 92,068). ^{1}H NMR ($CDCl_3$, 400 MHz) δ 0.89–0.93 (3H, m, C*H*$_3$), 1.31–1.44 (6H, m, $CH_3(CH_2)_3$), 1.67–1.74 (2H, m, $CH_3(CH_2)_3CH_2$), 2.82 (2H, t, $CH_3(CH_2)_4CH_2$, J = 7.4 Hz), 6.71 (1H, d, J = 3.2 Hz, 4″-H), 7.03 (1H, d, J = 3.2 Hz, 3″-H), 7.05 (1H, d, J = 3.6 Hz, 4′-H), 7.19 (1H, d, J = 3.6 Hz, 3′-H) 7.36 (1H, s, 6-H), 7.87 (1H, s, 3-H), 9.94 (1H, s, C*H*O) ppm. ^{13}C NMR ($CDCl_3$, 100.6 Hz) δ 14.1, 22.6, 28.7, 30.2, 31.5, 115.4, 115.5, 123.7, 124.1, 125.0, 126.1, 128.9, 133.8, 134.3, 137.4, 139.2, 144.5, 145.6, 146.6, 146.7, 182.9 ppm. MS (EI) *m/z* (%) = 416 ($[M]^+$, 28), 347 (13), 346 (13), 345 (100), 183 (10). HMRS: *m/z* (EI) found $[M]^+$ 416.0396; $C_{21}H_{20}OS_4$ requires 416.0397.

4.2.1.3. 5-(Furan-2'-yl)thieno[3,2-b]thiophene-2-carbaldehyde (**2c**).

Light brown solid (26%). Mp: 159–161 °C. IR (Nujol): 1650, 1305, 1233 cm-1 λ_{max}(ethanol)/nm 371 (ε/dm^3 mol^{-1} cm^{-1} 10,580). ^{1}H NMR ($CDCl_3$, 400 MHz) δ 6.52 (1H, dd, J = 3.4 and 1.6 Hz, 4′-H), 6.69 (1H, dd, J = 3.6 and 0.4 Hz, 5′-H), 7.45 (1H, d, J = 0.4 Hz, 6-H), 7.50 (1H, dd, J = 1.6 and 0.8 Hz, 3′-H), 7.89 (1H, d, J = 0.4 Hz, 3-H), 9.94 (1H, s, C*H*O) ppm. ^{13}C NMR ($CDCl_3$, 100.6 MHz) δ 107.78, 112.23, 114.67, 129.02, 137.55, 141.43, 143.16, 144.74, 146.54, 148.42, 182.97 ppm. MS (EI) *m/z* (%): 233 ($[M]^+$, 100), 232 (20), 205 (24), 176 (43). HMRS: *m/z* (EI) found $[M]^+$ 233.9807; $C_{11}H_6O_2S_2$ requires 233.9809.

4.2.1.4. 5-(N-Methylpyrrol-2'-yl)thieno[3,2-b]thiophene-2-carbaldehyde (**2d**).

Orange solid (84%). Mp: 108 °C (dec). IR (Nujol): 1652, 1548, 1233, 1206 cm^{-1} λ_{max}(ethanol)/nm 326 ε/dm^3 mol^{-1} cm^{-1} 4060). ^{1}H NMR (DMSO-d_6, 400 MHz) δ 3.81 (3H, s, N*CH*$_3$), 6.10 (1H, dd, J = 3.9 and 3.0 Hz, 3′-H), 6.44 (1H, dd, J = 3.9 and 1.8 Hz, 5′-H), 6.99 (1H, t, J = 2.1 Hz, 4′-H), 7.64 (1H, s, 6-H), 8.34 (1H, s, 3-H), 9.94 (1H, s, C*H*O) ppm. ^{13}C NMR (DMSO-d_6, 100.6 MHz) δ 35.5, 108.3, 111.3, 116.1, 126.1, 126.9, 131.3, 136.7, 143.3, 143.4, 145.9, 184.4 ppm. MS (EI) *m/z* (%) = 247 ($[M]^+$, 100), 246 (24), 218 (19), 176 (10), 69 (25). HMRS: *m/z* (EI) found $[M]^+$ 247.0129; $C_{12}H_9NOS_2$ requires 247.0126.

4.2.2. General procedure for the synthesis of thieno[3,2-b]thiophene derivatives **3** from the respective precursors **2** through Knoevenagel condensation

To a solution of aldehyde **2** (2.5 mmol) and 2-cyanoacetic acid (26 mg, 3 mmol) in ethanol was added 4 drops of piperidine. The mixture was refluxed for 6 h then cooled down to room temperature. The crude product was concentrated and ethyl ether was added to induce precipitation. The precipitate was filtered and washed with ethyl ether to give the pure product.

4.2.2.1. 2-Cyano-3-(2'-(thiophen-2″-yl)thieno[3,2-b]thiophen-5'-yl) acrylic acid (**3a**).

Orange solid (68%). Mp: 175–177 °C. IR (liquid film): 3426, 2305, 2190, 2096, 1634, 1265 cm^{-1} λ_{max}(ethanol)/nm 399 ε/dm^3 mol^{-1} cm^{-1} 31,288). ^{1}H NMR (DMSO-d_6, 400 MHz) δ 7.14 (1H, dd, J = 5.2 and 3.6 Hz, 4″-H), 7.43 (1H, dd, J = 3.6 and 1.2 Hz, 5″-H), 7.61 (1H, dd, J = 5.0 and 1.2 Hz, 3″-H), 7.76 (1H, s, 3′-H), 7.98 (1H, s, 6′-H), 8.12 (1H, s, 3-H), 8.85 (1H, s, O*H*) ppm. ^{13}C NMR (DMSO-d_6, 100.6 MHz) δ 109.39, 116.75, 119.19, 125.28, 126.89, 127.26, 128.63, 136.29, 137.03, 138.95, 140.97, 141.87, 143.44, 163.00 ppm. MS (ESI) *m/z* (%) = 318 ($[M+H]^+$, 100), 316 (59), 313 (39), 279 (61), 273 (41), 271 (39), 251 (37), 229 (34), 209 (31), 207 (95). HRMS: *m/z* (ESI) $[M+H]^+$ found 317.9712; $C_{14}H_8NO_2S_3$ requires 317.9717.

4.2.2.2. 2-Cyano-3-(2'-(5''-(5‴-hexylthiophen-2‴-yl)thiophen-2″-yl) thieno[3,2-b]thiophen-5'-yl)acrylic acid (**3b**).

Orange solid (43%). Mp: 202–204 °C. IR (liquid film): 3423, 2359, 2331, 2208, 2096, 1642 cm-1 λ_{max}(ethanol)/nm 433 (ε/dm^3 mol^{-1} cm^{-1} 16,574). ^{1}H NMR (DMSO-d_6, 400 MHz) δ 0.82–0.88 (3H, m, C*H*$_3$), 1.22–1.31 (6H, m, $CH_3(CH_2)_3$), 1.61–1.66 (2H, m, $CH_3(CH_2)_3CH_2$), 2.99 (2H, t, J = 5.6 Hz, $CH_3(CH_2)_4CH_2$), 6.83 (1H, d, J = 3.6 Hz, 4‴-H), 7.20 (1H, d, J = 3.6 Hz, 3‴-H), 7.24 (1H, d, J = 3.6 Hz, 4″-H), 7.42 (1H, d, J = 3.6 Hz, 3″-H), 7.81 (1H, s, 3′-H), 8.17 (1H, s, 6′-H), 8.39 (1H, s, 3-H) ppm. ^{13}C NMR (DMSO-d_6, 100.6 MHz) δ 13.9, 21.6, 22.21, 28.1, 30.9, 43.7, 116.7, 117.5, 124.5, 124.6, 125.9, 126.8, 130.6, 133.0, 134.0, 137.3, 137.7, 137.8, 143.3, 145.1, 145.9, 163.2, 163.4, 166.2 ppm. MS (ESI) *m/z* (%) = 531 (7), 513 (8), 500 (17), 499 (29), 498 (100), 497 (29), 484 ($[M+H]^+$, 7), 417 (20), 364 (8). HRMS: *m/z* (ESI) $[M+H]^+$ found 484.0528; $C_{24}H_{22}NO_2S_4$ requires 484.0533.

4.2.2.3. 2-Cyano-3-(2'-(furan-2″-yl)thieno[3,2-b]thiophen-5'-yl) acrylic acid (**3c**).

Orange solid (24%). Mp: 185–187° C. IR (liquid film): 3428, 2525, 2358, 2217, 2099, 1639 cm-1 λ_{max}(ethanol)/nm 398 (ε/dm^3 mol^{-1} cm^{-1} 32,084). ^{1}H NMR (DMSO-d_6, 400 MHz) δ 6.64 (1H, dd, J = 3.4 and 2.0 Hz, 4″-H), 6.93 (1H, d, J = 3.2 Hz, 5″-H), 7.77 (1H, s, 3′-H), 7.79 (1H, d, J = 2.0 Hz, 3″-H), 8.00 (1H, s, 6′-H), 8.13 (1H, s, 3-H), 9.00 (1H, brs, O*H*) ppm. ^{13}C NMR (DMSO-d_6, 100.6 MHz) δ 107.59, 109.09, 112.62, 115.52, 119.13, 127.44, 137.06, 137.80, 139.01, 141.10, 143.48, 143.65, 148.10, 163.15 ppm. MS (ESI) *m/z* (%) = 302 ($[M+H]^+$, 100), 296 (28), 279 (38), 273 (40), 271 (39), 207 (73). HRMS: *m/z* (ESI) $[M+H]^+$ found 301.9943; $C_{14}H_8NO_3S_2$ requires 301.9946.

*4.2.2.4. 2-Cyano-3-(2''-(N-methylpyrrol-2''-yl)thieno[3,2-b]thiophen-5'-yl)acrylic acid (**3d**).* Brown solid (11%). Mp. 183 °C (dec). IR (liquid film): 3411, 2359, 2328, 2213, 2098, 1638 cm-1 λ_{max}(-ethanol)/nm 364 (ε/dm^3 mol^{-1} cm^{-1} 38,948). ^{1}H NMR (DMSO-d_6, 400 MHz) δ 3.78 (3H, s, CH_3), 6.09 (1H, dd, J = 3.8 and 2.4 Hz, 4''-H), 6.39 (1H, dd, J = 3.6 and 1.6 Hz, 5''-H), 6.95 (1H, t, J = 2.2 Hz, 3''-H), 7.58 (1H, s, 3'-H), 7.96 (1H, s, 6'-H), 8.13 (1H, s, 3-H) ppm. ^{13}C NMR (DMSO-d_6, 100.6 MHz) δ 43.58, 108.10, 110.72, 116.24, 119.23, 126.26, 126.37, 127.37, 136.45, 137.96, 140.48, 141.36, 143.82, 163.57 ppm. MS (ESI) m/z (%) = 315 ([M+H]$^+$, 70), 313 (19), 280 (21), 279 (100), 257 (34). HRMS: m/z (ESI) [M+H]$^+$ found 315.0258; $C_{15}H_{11}N_2O_2S_2$ requires 315.0262.

4.3. Cyclic voltammetry

The measurements were performed using an AUTOLAB electrochemical station and a three electrode cell equipped with a vitreous carbon disc working electrode (3 mm), a platinum wire as counter-electrode and an Ag/AgCl electrode as reference electrode. The concentration of dyes was 1 mM with 1 mM of [NBu_4][BF_4] as supporting electrolyte in dry *N,N*-dymethylformamide solvent. The cyclic voltammetry was conducted at different scan-rates (20, 50, 100 and 200 mV s^{-1}) and the solutions were deoxygenated by bubbling nitrogen before each measurement. In non-aqueous solvents, the electrode potentials are often measured against the potential of the Fc^+/Fc redox couple [21].

4.4. DSSC preparation

A dye-sensitized solar cell consists of: i) TiO_2 photoelectrode where the dye molecules are adsorbed, both comprising the working electrode; ii) platinum counter-electrode; and iii) electrolyte containing the iodide/triiodide redox couple. To prepare the working electrodes, FTO glasses (TCO22-7, 2.2 mm thickness, 7 Ω/square, Solaronix, Switzerland) cleaned in a detergent solution using ultrasonic bath rinsed with water and dried at 60 °C were used. After treated in a UV- O_3 system for 15 min, the FTO substrates were immersed into a 40 mM aqueous $TiCl_4$ solution at 70 °C for 20 min and washed with ethanol and dried with N_2. A layer of TiO_2 paste (Ti-Nanoxide T/SP, Solaronix, Switzerland) was coated on the FTO glass by screen-printing, kept at room temperature for 20 min and then dried for 5 min at 120 °C. The screen-printing procedure was repeated 2 more times, in order to reach 3 layers of TiO_2 paste (0.2 cm^2 of circular active area, and 12 μm of thickness). After drying the photoelectrode at 120 °C, it was gradually heated (10 °C min^{-1}) up to 475 °C for 30 min. The TiO_2 electrode was then immersed into a 0.5 mM dye solution in ethanol and kept at room temperature for 12 h.

To prepare the counter electrodes, two holes were drilled in the FTO glass with a drilling machine with diamond tip. The FTO substrates were then washed as described before. Pt catalyst (Platisol T/SP, Solaronix, Switzerland) was deposited on the FTO side of the glass by screen-printing and then heated up to 450 °C for 10 min.

The dye-covered TiO_2 electrode and the Pt counter-electrode were assembled into a sandwich type cell and sealed with a hot-melt gasket of 25 μm thickness – Surlyn (Meltonix 1170-25, Solaronix, Switzerland) by hot-pressing. The electrolyte (Iodolyte AN-50, Solaronix, Switzerland) was injected into the cell through the holes presented in the counter-electrode side. These holes were then sealed by Surlyn® and a cover glass using a soldering iron.

4.5. Photovoltaic performance measurements

A 150 W Xenon light source (Oriel class a solar simulator, Newport, USA) was used to give an irradiance of 100 mW cm^{-2} (equivalent of one sun at AM 1.5G) at the surface of solar cells. The simulator was calibrated using a single crystal Si photodiode (Newport, USA). The current-voltage characteristics of the cell under these conditions were obtained applying an external potential bias to the cell and measuring the generated photocurrent with ZENNIUM workstation (Ref. 2425-C, Zahner Elektrik, Germany). Photovoltaic performance was measured using a metal mask with an aperture area of 0.2 cm^2.

Acknowledgments

Thanks are due to: *Fundação para a Ciência e Tecnologia* (FCT) for PhD grants to S. S. M. Fernandes (SFRH/BD/87786/2012), M. C. R. Castro (SFRH/BD/78037/2011) and I. Mesquita (PD/BD/105985/2014); FEDER-COMPETE for financial support through the Centro de Química PEst-C/QUI/UI0686/2011 (F-COMP-01-0124-FEDER-022716); European Research Council (Contract no: 321315) for funding. The NMR spectrometer Bruker Avance III 400 is part of the National NMR Network and was purchased within the framework of the National Program for Scientific Re-equipment, contract REDE/1517/RMN/2005 with funds from POCI 2010 (FEDER) and FCT.

References

[1] (a) O'Regan B, Grätzel M. A low-cost, high-efficiency solar cell based on dye-sensitized colloidal TiO_2 films. Nature 1991;353:737–40.
(b) Grätzel M. Dye-sensitized solar cells. J Photochem Photobiol C 2003;4:145–53.
c) Grätzel M. Conversion of sunlight to electric power by nanocrystalline dye-sensitized solar cells. J Photochem Photobiol A 2004;164:3–14.
d) Grätzel M. Recent advances in sensitized mesoscopic solar cells. Acc Chem Res 2009;42:1788–98.
e) Yella A, Lee H-W, Tsao HN, Yi C, Chandiran AK, Nazeeruddin MK, et al. Porphyrin-sensitized solar cells with cobalt (ii/iii)–based redox electrolyte exceed 12 percent efficiency. Science 2011;334:629–34.
(f) Bignozzi CA, Argazzi R, Boaretto R, Busatto E, Carli S, Ronconi F, et al. The role of transition metal complexes in dye sensitized solar devices. Coord Chem Rev 2013;257:1472–92.

[2] a) Maçaira J, Andrade L, Mendes A. Modeling, simulation and design of dye sensitized solar cells. RSC Adv 2014;4:2830–44.
(b) Maçaira J, Andrade L, Mendes A. Review on nanostructured photoelectrodes for next generation dye-sensitized solar cells. Renew Sustain Energy Rev 2013;27:334–49.
c) Gonçalves LM, de Zea Bermudez V, Ribeiro HA, Mendes AM. Dye-sensitized solar cells: a safe bet for the future. Energy Environ Sci 2008;1:655–67.

[3] (a) Robertson N. Optimizing dyes for dye-sensitized solar cells. Angew Chem Int Ed 2006;45:2338–45.
(b) Mishra A, Fischer MKR, Bäuerle P. Metal-free organic dyes for dye-sensitized solar cells: from structure: property relationships to design rules. Angew Chem Int Ed 2009;48:2474–99.
(c) Ooyama Y, Harima Y. Molecular designs and syntheses of organic dyes for dye-sensitized solar cells. Eur J Org Chem 2009;18:2903–34.
(d) Hagfeldt A, Boschloo G, Sun L, Kloo L, Pettersson H. Dye-sensitized solar cells. Chem Rev 2010;110:6595–663.
e) Ning Z, Fu Y, Tian H. Improvement of dye-sensitized solar cells: what we know and what we need to know. Energy Environ Sci 2010;3:1170–81.
f) Clifford JN, Martinez-Ferrero E, Viterisi A, Palomares E. Sensitizer molecular structure-device efficiency relationship in dye sensitized solar cells. Chem Soc Rev 2011;40:1635–46.
(g) Yen Y-S, Chou H-H, Chen Y-C, Hsu C-Y, Lin JT. Recent developments in molecule-based organic materials for dye-sensitized solar cells. J Mater Chem 2012;22:8734–47.
(h) Ooyama Y, Harima Y. Photophysical and electrochemical properties, and molecular structures of organic dyes for dye-sensitized solar cells. ChemPhysChem 2012;13:4032–80.
(i) Kanaparthi RK, Kandhadi J, Giribabu L. Metal-free organic dyes for dye-sensitized solar cells: recent advances. Tetrahedron 2012;68:8383–93.
(j) Kim B-G, Chung K, Kim J. Molecular design principle of all-organic dyes for dye-sensitized solar cells. Chem Eur J 2013;19:5220–30.
(k) Wu Y, Zhu W. Organic sensitizers from d-π-a to d-a-π-a: effect of the internal electron-withdrawing units on molecular absorption, energy levels and photovoltaic performances. Chem Soc Rev 2013;42:2039–58.
(l) Ahmad S, Guillén E, Kavan L, Grätzel M, Nazeeruddin MK. Metal free sensitizer and catalyst for dye sensitized solar cells. Energy Environ Sci 2013;6:3439–66.
(m) Zhang L, Cole JM. Anchoring groups for dye-sensitized solar cells. ACS Appl Mater Interfaces 2015;7:3427–55.

(n) Mahmood A. Triphenylamine based dyes for dye sensitized solar cells: a review. Sol Energy 2016;123:127–44.

[4] (a) Wan Z, Jia C, Duan Y, Zhang J, Lin Y, Shi Y. Effects of different acceptors in phenothiazine-triphenylamine dyes on the optical, electrochemical, and photovoltaic properties. Dyes Pigm 2012;94:150–5.
(b) Ramkumar S, Manoharan S, Anandan S. Synthesis of d-(π-a)$_2$ organic chromophores for dye-sensitized solar cells. Dyes Pigm 2012;94:503–11.
(c) Song J-L, Amaladass P, Wen S-H, Pasunooti KK, Li A, Yu Y-L, et al. Aryl/hetero-arylethyne bridged dyes: the effect of planar π-bridge on the performance of dye-sensitized solar cells. New J Chem 2011;35:127–36.
(d) Ma XM, Wu WJ, Zhang Q, Guo FL, Meng FS, Hua. Novel fluoranthene dyes for efficient dye-sensitized solar cells. Dyes Pigm 2009;82:353–9.
(e) Marinado T, Hagberg DP, Hedlund M, Edvinsson T, Johansson EMJ, Boschloo G. Rhodanine dyes for dye-sensitized solar cells: spectroscopy, energy levels and photovoltaic performance. Phys Chem Chem Phys 2009;11:133–41.

[5] (a) Choi H, Baik C, Kang SO, Ko J, Kang M-S, Nazeeruddin MK, et al. Highly efficient and thermally stable organic sensitizers for solvent-free dye-sensitized solar cells. Angew Chem 2008;120:333–6.
(b) Zhang G, Bala H, Cheng Y, Shi D, Lv X, Yu Q, et al. High efficiency and stable dye-sensitized solar cells with an organic chromophore featuring a binary π-conjugated spacer. Chem Commun 2009;16:2198–200.
(c) Choi H, Raabe I, Kim D, Teocoli F, Kim C, Song K, et al. High molar extinction coefficient organic sensitizers for efficient dye-sensitized solar cells. Chem Eur J 2010;16:1193–201.
(d) Paek S, Choi H, Choi H, Lee C-W, M-s Kang, Song K, et al. Molecular engineering of efficient organic sensitizers incorporating a binary π-conjugated linker unit for dye-sensitized solar cells. J Phys Chem C 2010;114:14646–53.
(e) Tsao HN, Burschka J, Yi C, Kessler F, Nazeeruddin MK, Grätzel M. Influence of the interfacial charge-transfer resistance at the counter electrode in dye-sensitized solar cells employing cobalt redox shuttles. Energy Environ Sci 2011;4:4921–4.
(f) Metri N, Sallenave X, Plesse C, Beouch L, Aubert P-H, Goubard F, et al. Processable star-shaped molecules with triphenylamine core as hole-transporting materials: experimental and theoretical approach. J Phys Chem C 2012;116:3765–72.
[g] Wu Y, Marszalek M, Zakeeruddin SM, Zhang Q, Tian H, Gratzel M, et al. High-conversion-efficiency organic dye-sensitized solar cells: molecular engineering on d-a-π-a featured organic indoline dyes. Energy Environ Sci 2012;5:8261–72.
(h) Cai S, Tian G, Li X, Su J, Tian H. Efficient and stable DSSC sensitizers based on substituted dihydroindolo[2,3-*b*]carbazole donors with high molar extinction coefficients. J Mater Chem A 2013;1:11295–305.
(i) Gao P, Tsao HN, Yi C, Graetzel M, Nazeeruddin MK. Extended π-bridge in organic dye-sensitized solar cells: the longer, the better? Adv Energy Mater 2014;4:1–7.
(j) Kakiage K, Aoyama Y, Yano T, Otsuka T, Kyomen T, Unno M, et al. An achievement of over 12 percent efficiency in an organic dye-sensitized solar cell. Chem Commun 2014;50:6379–81.
(k) Lee M-W, Kim J-Y, Lee D-H, Ko MJ. Novel D-π-A organic dyes with thieno[3,2-*b*]thiophene-3,4-ethylenedioxythiophene unit as a π-bridge for highly efficient dye-sensitized solar cells with long-term stability. ACS Appl Mater Interfaces 2014;6:4102–8.
(l) Kakiage K, Aoyama Y, Yano T, Oya K, Fujisawab JI, Hanaya M. Highly-efficient dye-sensitized solar cells with collaborative sensitization by silyl-anchor and carboxy-anchor dyes. Chem Comm 2015;51:15894–7.

[6] (a) Cinar ME, Ozturk T. Thienothiophenes, dithienothiophenes, and thienoacenes: syntheses, oligomers, polymers, and properties. Chem Rev 2015;115:3036–140.
(b) Liu H, Wu F, Zhao B, Meng L, Wang G, Zhang J, et al. Synthesis and photovoltaic properties of the acceptor pended push–pull conjugated polymers incorporating thieno[3,2-*b*] thiophene in the backbone chain or side chains. Dyes Pigm 2015;120:44–51.
(c) Zhu S, An Z, Sun X, Wu Z, Chen X, Chen P. Synthesis and evaluation of simple molecule as a co-adsorbent dye for highly efficient co-sensitized solar cells. Dyes Pigments 2015;120:85–92.
(d) Brogdon P, Giordano F, Puneky GA, Dass A, Zakeeruddin SM, Nazeeruddin MK, et al. A computational and experimental study of thieno[3,4-*b*]thiophene as a proaromatic pi-bridge in dye-sensitized solar cells. Chem Eur J 2016;22:694–703.
(e) Chen Y-C, Chou H-H, Tsai MC, Chen S-Y, Lin JT, Yao C-F, et al. Thieno[3,4-b] thiophene-based organic dyes for dye-sensitized solar cells. Chem Eur J 2012;18:5430–7.

[7] (a) Raposo MMM, Castro MCR, Belsley M, Fonseca AMC. Push–pull bithiophene azo-chromophores bearing thiazole and benzothiazole acceptor moieties: synthesis and evaluation of their redox and nonlinear optical properties. Dyes Pigments 2011;91:454–65.
(b) Genin E, Hugues V, Clermont G, Herbivo C, Castro MCR, Comel A, et al. Fluorescence and two-photon absorption of push-pull aryl(bi)thiophenes: structure-property relationships. Photochem Photobiol Sci 2012;11:1756–66.
(c) Castro MCR, Belsley M, Fonseca AMC, Raposo MMM. Synthesis and characterization of novel second-order NLO-chromophores bearing pyrrole as an electron donor group. Tetrahedron 2012;68:8147–55.
(d) Pina J, Seixas de Melo JS, Batista RMF, Costa SPG, Raposo MMM. Triphenylamine–benzimidazole derivatives: synthesis, excited-state characterization, and DFT studies. J Org Chem 2013;78:11389–95.
(e) Garcia-Amorós J, Reig M, Castro MCR, Cuadrado A, Raposo MMM, Velasco D. Molecular photo-oscillators based on highly accelerated heterocyclic azo dyes in nematic liquid crystals. Chem Commun 2014;50:6704–6.
(f) Batista RMF, Costa SPG, Raposo MMM. Selective colorimetric and fluorimetric detection of cyanide in aqueous solution using novel heterocyclic imidazo-anthraquinones. Sensors Actuators B Chem 2014;191:791–9.
g) Castro MCR, Belsley M, Raposo MMM. Push-pull second harmonic generation (SHG) chromophores bearing pyrrole and thiazole heterocycles functionalized with strong acceptor moieties: syntheses and characterization. Dyes Pigments 2016;128:89–95.

[8] (a) Raposo MMM, Sousa AMRC, Kirsch G, Cardoso P, Belsley M, de Matos Gomes E, et al. Synthesis and characterization of dicyanovinyl-substituted thienylpyrroles as new nonlinear optical chromophores. Org Lett 2006;8:3681–4.
(b) Batista RMF, Costa SPG, Belsley M, Lodeiro C, Raposo MMM. Synthesis and characterization of novel (oligo)thienyl-imidazo-phenanthrolines as versatile π-conjugated systems for several optical applications. Tetrahedron 2008;64:9230–8.
(c) Batista RMF, Costa SPG, Malheiro EL, Belsley M, Raposo MMM. Synthesis and characterization of new thienylpyrrolyl-benzothiazoles as efficient and thermally stable nonlinear optical chromophores. Tetrahedron 2007;63:4258–65.

[9] Tejada RP, Pelleja L, Palomares E, Franco S, Orduna J, Garin J, et al. Novel 4H-pyranylidene organic dyes for dye-sensitized solar cells: effect of different heteroaromatic rings on the photovoltaic properties. Org Electron 2014;15:3237–50.

[10] Raposo MMM, Fonseca AMC, Castro MCR, Belsley M, Cardoso MFS, Carvalho LM, et al. Synthesis and characterization of novel diazenes bearing pyrrole, thiophene and thiazole heterocycles as efficient photochromic and nonlinear optical (NLO) materials. Dyes Pigm 2011;91:62–73.

[11] Kim BH, Freeman HS. New N-methyl pyrrole and thiophene based d–π–a systems for dye-sensitized solar cells. Dyes Pigments 2013;96:313–8.

[12] Horiuchi T, Miura H, Uchida S. Highly-efficient metal-free organic dyes for dye-sensitized solar cells. Chem Commun 2003;24:3036–7.

[13] Wang P, Klein C, Humphry-Baker R, Zakeeruddin SM, Grätzel M. A high molar extinction coefficient sensitizer for stable dye-sensitized solar cells. J Am Chem Soc 2005;127:808–9.

[14] Pina J, Seixas de Melo JS, Batista RMF, Costa SPG, Raposo MMM. Synthesis and characterization of the ground and excited states of tripodal-like oligothienylimidazoles. J Phys Chem B 2010;114:4964–72.

[15] Hagfeldt A, Graetzel M. Light-induced redox reactions in nanocrystalline systems. Chem Rev 1995;95:49–68.

[16] (a) Al-Eid M, Lim S, Park K-W, Fitzpatrick B, Han C-H, Kwak K, et al. Facile synthesis of metal-free organic dyes featuring a thienylethynyl spacer for dye sensitized solar cells. Dyes Pigm 2014;104:197–203.
(b) Pellejà L, Dominguez R, Aljarilla A, Clifford JN, de la Cruz P, Langa F, et al. Use of thienylenevinylene and ethynyl molecular bridges in organic dyes for dye-sensitized solar cells: implications for device performance. ChemElectroChem 2014;1:1126–9.
(c) Mikroyannidis JA, Tsagkournos DV, Balraju P, Sharma GD. Low band gap dyes based on 2-styryl-5-phenylazo-pyrrole: synthesis and application for efficient dye-sensitized solar cells. J Power Sources 2011;196:4152–61.

[17] (a) He J, Wu W, Hua J, Jiang Y, Qu S, Li J, et al. Bithiazole-bridged dyes for dye-sensitized solar cells with high open circuit voltage performance. J Mater Chem 2011;21:6054–62.
(b) Koumura N, Wang Z-S, Mori S, Miyashita M, Suzuki E, Hara K. Alkyl-functionalized organic dyes for efficient molecular photovoltaics. J Am Chem Soc 2006;128:14256–7.

[18] Morris JV, Mahaney MA, Huber JR. Fluorescence quantum yield determinations. 9,10-diphenylanthracene as a reference standard in different solvents. J Phys Chem 1976;80:969–74.

[19] Collado D, Remón P, Vida Y, Najera F, Sen P, Pischel U, et al. Energy transfer in aminonaphthalimide-boron-dipyrromethene (bodipy) dyads upon one- and two-photon excitation: applications for cellular imaging. Chem - Asian J 2014;9:797–804.

[20] Herbivo C, Comel A, Kirsch G, Raposo MMM. Synthesis of 5-aryl-5′-formyl-2,2′-bithiophenes as new precursors for nonlinear optical (nlo) materials. Tetrahedron 2009;65:2079–86.

[21] Cardona CM, Li W, Kaifer AE, Stockdale D, Bazan GC. Electrochemical considerations for determining absolute frontier orbital energy levels of conjugated polymers for solar cell applications. Adv Mater 2011;23:2367–71.